Cascaded dynamics of a periodically driven dissipative dipolar system

Saptarshi Saha [*] and Rangeet Bhattacharyya [†]

Department of Physical Sciences, Indian Institute of Science Education and Research Kolkata, Mohanpur 741 246, West Bengal, India

Recent experiments show that periodic drives on dipolar systems lead to long-lived prethermal states. These systems are weakly coupled to the environment and reach prethermal states on a timescale much shorter than the timescale for thermalization. Such nearly closed systems have previously been analyzed using Floquet formalism, which shows the emergence of a prethermal plateau. We use a fluctuation-regulated quantum master equation (FRQME) to describe these systems. In addition to the system-environment coupling, FRQME successfully captures the dissipative effect from the various local interactions in the system. Our investigation reveals a cascaded journey of the system to a final steady state. The cascade involves a set of prethermal or arrested states characterized by a set of quasiconserved quantities. We show that these prethermal states emerge in a timescale much shorter than the relaxation timescale. We also find and report the existence of a critical limit beyond which the prethermal plateau ceases to exist.

I. INTRODUCTION

Experimental evidence shows that nearly isolated systems exhibit prethermalization on a timescale much shorter than that expected from the system-environment coupling [1,2]. A complete understanding of how such nearly isolated systems reach a thermal state remains an enigma. The understanding of the dynamics of this process is now at the forefront of quantum and statistical mechanics research [3,4]. Earlier, Deutsch showed an approach to thermalization in a microcanonical ensemble might be realized through the inclusion of a random Hamiltonian in the system [3,5]. Another major milestone in the understanding of the thermalization process came from Srednicki; he proposed separate thermalization within the subspace of each eigenvalue of the system, known as the eigenstate thermalization hypothesis (ETH) [6,7]. In the process of thermalization, the system may encounter long-duration prethermal states at an intermediate timescale. Such prethermal states are characterized by incomplete loss of initial memory, as opposed to the complete loss in a thermalization process [4].

For isolated many-body quantum systems, under some circumstances, a periodic drive can lead the system to the long-lived prethermal plateau. It has been theoretically analyzed using Floquet theory and is known as Floquet prethermalization [8–14]. The prethermal plateau has a large number of applications in quantum computation, information processing, and quantum state engineering [15]. Experimental demonstrations of Floquet prethermalization are opening a new frontier in nonequilibrium quantum physics [16–20].

We note that a recently introduced fluctuation-regulated quantum master equation (FRQME) is capable of describing the nonequilibrium dynamics of a nearly closed system in a unique way by taking into account the dissipators from system interactions in addition to the system-environment coupling [21]. The unique feature in FRQME is the addition of an explicit bath fluctuation term in the dynamics. While the system evolves infinitesimally under the system Hamiltonians, the bath undergoes a finite propagation under fluctuations. This composite propagation results in a Markovian master equation with a memory kernel in all dissipator terms [21]. FRQME has been used as an essential tool for theoretical analysis of drive-induced effects in quantum optics, quantum information processing, and nuclear magnetic resonance (NMR) [22–26].

For a driven dipolar dissipative system, in addition to the first-order effects, one can have dissipators from a drive, dipolar relaxation terms, and their cross terms, all potentially much larger than the relaxation terms from system-environment coupling [27]. Naturally, FRQME can describe the dynamics of nearly closed systems at an intermediate timescale when the above condition is met. We shall show that the dynamics of such a system is dominated by terms other than the relaxation terms, and the journey to the final steady state may have multiple timescales.

In the following, we analyze such a system as a prototype closed system by keeping the system-environment coupling vanishingly small compared to the other terms in the equation. We obtain a set of quasiconserved quantities which aid in evolving the system from the initial state to the final steady state punctuated by one or more prethermal plateau or an *arrested state*. Each prethermal state is characterized by quasiconserved quantities and the decay of each plateau is associated with the breaking of these quasiconservation laws.

We organize the paper in the following order. In Sec. II, we provide a brief description of the system, where a dipolar coupled two-spin system is weakly coupled with the local environment and a weak on-resonant periodic drive is applied

* ss17rs021@iiserkol.ac.in
† rangeet@iiserkol.ac.in

in the system. Using FRQME, the full dynamical evolution of the system is shown in Sec. III. In this section, we also analyze the dynamical behavior by using three subsection. In Sec. III A, we show the emergence of a prethermal plateau. The dynamics of constrained thermalization and the existence of a critical limit are discussed in Secs. III B and III B 1. The dynamical behavior of unconstrained thermalization is demonstrated in Sec. III C. Then, we analyze the results and discuss the implications of the cascaded dynamics in Sec. IV. Finally, we discuss the merits and the demerits of our approach and draw conclusions in Sec. V.

II. DESCRIPTION OF THE SYSTEM

We consider two dipolar coupled spin-1/2 particles with the same Zeeman splitting. They are periodically driven. The individual spins are weakly coupled with the external thermal environment that is undergoing fluctuations with characteristic timescale τ_c. Except for the fluctuations, the rest of the model mimics the experimental condition at which Beatrez *et al.* observed a prethermal plateau [18].

The total Hamiltonian of the system and its environment is given by

$$\mathcal{H}(t) = \mathcal{H}_S^\circ + \mathcal{H}_L^\circ + \mathcal{H}_{SL} + \mathcal{H}_{DD} + \mathcal{H}_{DR}(t) + \mathcal{H}_L(t). \quad (1)$$

Here, the first two terms are the free Hamiltonians of the system and local environment. $\mathcal{H}_S^\circ$ represents the Zeeman interaction and the form is given by $\sum_{i=1}^{2} \omega_\circ I_z^i$, where $\omega_\circ$ is the Zeeman frequency. Here $I_\alpha^i = \sigma_\alpha^i / 2$, $\alpha \in \{x, y, z\}$, σ_α is α component of Pauli spin operators for spin-1/2 particles, and i is the spin index. For the environment, from its multitude of levels, we choose the two resonant levels having $\omega_L \approx \omega_\circ$ energy spacing. As such, we define $\mathcal{H}_L^\circ = \omega_L L_+ L_-$, where ω_L is the frequency of $\mathcal{H}_L^\circ$ and $L_\pm$ are the corresponding creation and annihilation operators of the local environment of each spin. Therefore, the bath is modeled as a single large quantum object that provides the necessary dissipation to the system. $\mathcal{H}_{SL}$ depicts the system-local environment coupling Hamiltonian, which provides the relaxation terms. Following the Jaynes-Cummings model, the form of $\mathcal{H}_{SL}$ is chosen as

$$\mathcal{H}_{SL} = \sum_{i=1}^{2} \omega_{SL}(I_+^i L_-^i + \text{H.c.}). \quad (2)$$

Here, ω_{SL} is the system-local environment coupling amplitude. i is the spin index.

The next term in the list of Hamiltonians is the dipolar coupling; its analytical form in spherical tensor notation is given by $\mathcal{H}_{DD} = \sum_{m=-2}^{2} (-1)^m \omega_{d_m} \mathcal{T}_2^m$, where $\omega_{d_m} = (\mu_\circ \hbar \gamma^2 / 4\pi r^3) \, \mathcal{Y}_2^{-m}(\theta, \phi)$. $\mathcal{Y}_2^{-m}(\theta, \phi)$ is the spherical harmonics of rank 2, and $\mathcal{T}_2^m$ is the irreducible spherical tensor (of rank 2 and order m). (θ, ϕ) are the polar and azimuthal angles of the average orientation of the dipolar vector with regard to the direction of the magnetic field. γ is the gyro-magnetic ratio of the spin and $\mu_\circ$ is the permeability constant. $\vec{r}$ is the average distance between the two spins [28]. A weak, linearly polarized, and periodic drive is applied in the transverse direction of the system. The corresponding drive Hamiltonian is written as $\mathcal{H}_{DR}(t) = \sum_{i=1}^{2} \omega_1 I_x^i \cos \omega t$. Here, the drive frequency is $\omega = \omega_\circ$, as we consider an on-resonant periodic excitation.

$\mathcal{H}_L(t)$ represents the spontaneous thermal fluctuation in the local environment which eventually provides a memory kernel in the dissipator [21]. The form is chosen as $\mathcal{H}_L(t) = \sum_i f_i(t) |\phi_i\rangle\langle\phi_i|$, where $\{|\phi_i\rangle\}$ are the eigenbasis of the environment. f_i are the independent Gaussian stochastic variables with zero mean and standard deviation κ ($\kappa^2 = \frac{1}{\tau_c}$), where τ_c is the correlation time. This specific choice of $\mathcal{H}_L(t)$ ensures that the explicit presence of the thermal fluctuation does not destroy the equilibrium density matrix of the environment, but it does destroy the coherences in the environment with a timescale τ_c.

III. DYNAMICAL EQUATION

We assume that a clear timescale separation exists, i.e., τ_c is much smaller than the system's timescale. Then one can construct a propagator that evolves the system infinitesimally and evolves the environment under fluctuations by a finite amount. A coarse-graining followed by a cumulant expansion of the fluctuation part of the propagator results in a Markovian quantum master equation with a memory kernel in all its dissipators [21]. For the case in hand, the dynamical equation of the reduced system density matrix—the FRQME—in the interaction picture of the free Hamiltonians $\mathcal{H}_S^\circ + \mathcal{H}_L^\circ$ is given by

$$\frac{d\rho_S}{dt} = -i\text{Tr}_L[H_{\text{eff}}(t), \rho_S \otimes \rho_L^{\text{eq}}]^{\text{sec}}$$
$$- \int_0^\infty d\tau \text{Tr}_L[H_{\text{eff}}(t), [H_{\text{eff}}(t - \tau), \rho_S \otimes \rho_L^{\text{eq}}]]^{\text{sec}} e^{-\frac{|\tau|}{\tau_c}}, \quad (3)$$

where $H_{\text{eff}}(t)$ is the interaction representation of $\mathcal{H}_{SL} + \mathcal{H}_{DR}(t) + \mathcal{H}_{DD}(t)$. ρ_L^{eq} is the equilibrium density matrices of the environment. On the right-hand side, "sec" denotes the secular approximation [29]. We note the presence of the exponential kernel ($\exp(-t/\tau_c)$), which gives a finite second-order effect of any local Hamiltonian (e.g., $\mathcal{H}_{DR}(t)$ and $\mathcal{H}_{DD}$) along with $\mathcal{H}_{SL}$.

In the interaction picture, the drive and dipolar Hamiltonian can be written as the sum of the secular (time-independent) and nonsecular (time-dependent) parts. The analytical form of the secular parts is given by $H_{DR}^{\text{sec}} = \omega_1 \sum_i I_x^i$ and $H_{DD}^{\text{sec}} = \omega_{d_0} \mathcal{T}_2^0$. Similarly the nonsecular parts are written as $H_{DD}^{\text{n}} = \sum_m (-1)^m \omega_{d_m} \mathcal{T}_2^m e^{-im\omega_\circ t} \quad [\forall m \neq 0]$, $H_{DR}^{\text{n}} = \sum_i \omega_1 (I_+^i e^{+2i\omega_\circ t} + I_-^i e^{-2i\omega_\circ t})$. In the superscript, "sec" denotes the secular part, and "n" denotes the nonsecular part of the Hamiltonian. We note that the effect of the secular components is much stronger than that of the nonsecular component in the dynamics, as the secular parts are present in the first-order commutator, whereas the nonsecular components are only present in the dissipators.

In Liouville space, the dynamical equation can be written as $\frac{d\hat{\rho}_S(t)}{dt} = \hat{\mathcal{L}}\hat{\rho}_S(t)$. For our case, $\hat{\mathcal{L}}$ is a 16×16 matrix and $\hat{\rho}_S$ is a 16×1 column matrix. The detailed form of $\hat{\mathcal{L}}\hat{\rho}_S$ is given by $\hat{\mathcal{L}}\hat{\rho}_S = (\hat{\mathcal{L}}_{\text{sec}} + \hat{\mathcal{L}}_n + \hat{\mathcal{L}}_{SL})\hat{\rho}_S$. The three terms, $\hat{\mathcal{L}}_{\text{sec}}$, $\hat{\mathcal{L}}_n$, $\hat{\mathcal{L}}_{SL}$ denote the Liouvillian corresponding to the secular parts,
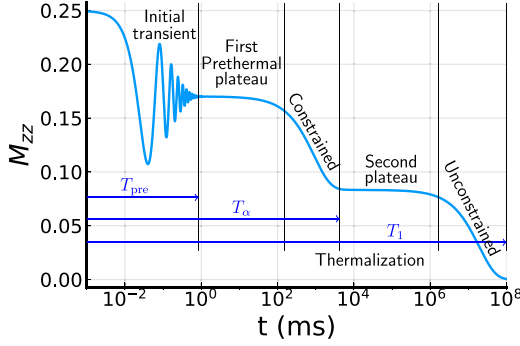
FIG. 1. The plot shows the complete dynamics of the observable M_{zz} as a function of t in log scale. The plot was generated by solving FRQME in Eq. (3) for $\omega_1 = 2\pi \times 5$ KHz, $|\omega_{dm}| = 2\pi \times 5$ KHz, $\omega_\circ = 2\pi \times 10$ MHz, $\tau_c = 1$ μs, $T_1 = 5 \times 10^7$ ms, and $M_{zz}|_{t\to 0} = \frac{1}{4}$. The choice of parameters ensures that regular relaxation comes into play long after the other dissipators have completed their part. The dynamics clearly show the emergence of multiple prethermal states and the cascaded journey to the final steady state. T_{pre} shows the timescale at which the initial transients die out and the first prethermal state emerges. This state further decays under a constrained thermalization process, and the second prethermal plateau emerges after T_α. The regular relaxation with a longer timescale T_1 finally takes the system to a steady state.

the nonsecular parts, and system-bath coupling Hamiltonian respectively.

Instead of working with a full density matrix, we chose to rewrite the equation in terms of the expectation values of the relevant spin observables, which can be easily interpreted to gain insight into the dynamics. Normally, a two-spin density matrix can be written by using 15 observables. For a symmetric case, the number of observables is reduced to nine. The representation of $\rho_s(t)$ is given by

$$\rho_s(t) = \sum_{\alpha,\beta} A_{\alpha\beta} I_\alpha \otimes I_\beta, \qquad (4)$$

where α, β can take values from $\{x, y, z, d\}$, and $I_d = 2 \times 2$ identity matrix. Here, we further define $M_i = A_{id} + A_{di}$, $M_{ii} = A_{ii}$, $M_{ij} = A_{ij} + A_{ji}$ $\forall i \neq j$, and $i, j \neq d$.

First, we show the complete solution of Eq. (3) in terms of one of the observables defined in Eq. (4) for the initial condition, $\rho_s|_{t\to 0} = |\uparrow\uparrow\rangle\langle\uparrow\uparrow|$ i.e., $M_{zz}|_{t\to 0} = \frac{1}{4}$) in Fig. 1. A detailed discussion on the choice of the initial state is provided later. The figure caption contains the parameters used for generating the plot. The expressions of T_1, T_{pre}, T_α are also given later. We observe a cascaded journey of this observable from the initial value to the final steady state. We shall analyze the cascaded evolution by systematically including various interactions with decreasing strengths.

A. Emergence of the prethermal plateau

We note that Chakrabarti *et al.* has recently described the emergence of prethermal plateau [27], and hence we provide a brief review here. One needs to consider the strongest Liouvillian ($\hat{\mathcal{L}}_{\text{sec}}$) to understand the dynamics. Only the effect of the secular parts are considered here ($H_{\text{tot}}^{\text{sec}} = H_{\text{DR}}^{\text{sec}} + H_{\text{DD}}^{\text{sec}}$).

The explicit form of $\hat{\mathcal{L}}_{\text{sec}}\hat{\rho}_s$ in the Hilbert space is given below,

$$\mathcal{L}_{\text{sec}}\rho_s = -i\big[H_{\text{tot}}^{\text{sec}}, \rho_s\big] - \tau_c\big[H_{\text{tot}}^{\text{sec}}, \big[H_{\text{tot}}^{\text{sec}}, \rho_s\big]\big]. \qquad (5)$$

Drive and dipolar interaction can appear in both first order and second order of the above Eq. (5). Cross relaxation occurs due to the cross terms of $H_{\text{DR}}^{\text{sec}}$ and $H_{\text{DD}}^{\text{sec}}$ in the second order.

The dynamical equation for the collective coherence (M_x) and corresponding coupled observables which are connected to the quasiconserved quantities are written as

$$\dot{M}_x = -\tfrac{9}{4}\omega_{d_0}^2\tau_c M_x + 6\omega_1\omega_{d_0}\tau_c M_{zz} - 6\omega_1\omega_{d_0}\tau_c M_{yy} - 3\omega_{d_0}M_{yz}, \qquad (6)$$

$$\dot{M}_{zz} = \tfrac{3}{4}\omega_1\omega_{d_0}\tau_c M_x - 2\omega_1^2\tau_c M_{zz} + 2\omega_1^2\tau_c M_{yy} + \omega_1 M_{yz}, \qquad (7)$$

$$\dot{M}_{yy} = -\tfrac{3}{4}\omega_1\omega_{d_0}\tau_c M_x + 2\omega_1^2\tau_c M_{zz} - 2\omega_1^2\tau_c M_{yy} - \omega_1 M_{yz}, \qquad (8)$$

$$\dot{M}_{yz} = \tfrac{3}{4}\omega_{d_0}M_x - 2\omega_1 M_{zz} + 2\omega_1 M_{yy} - \big(4\omega_1^2 + \tfrac{9}{4}\omega_{d_0}^2\tau_c\big)M_{yz}. \qquad (9)$$

We note that the above equations show several constants of motion. For example, from the above, we infer, $M_{yy} + M_{zz}$, $3\omega_{d_0}M_{zz} + \omega_1 M_x$ are constants. From the other equations (not shown), we also have $\dot{M}_{xx} = 0$, and hence M_{xx} is also a conserved quantity. However, as one includes other nonsecular terms, these quantities may not remain conserved. But being weaker than secular parts, the effect of nonsecular terms becomes evident in the later part of the dynamics. As such, these quantities appear to be constant for a while and then undergo changes. Following Peng *et al.*, we term these quantities as quasiconserved [19]. Since the presence of the coherence M_x as an arrested state was observed recently by Beatrez *et al.* [18], we name the quasiconserved quantity $3\omega_{d_0}M_{zz} + \omega_1 M_x$ as the prethermal order. Similarly, we have another quasiconserved quantity $M_{xx} + M_{yy} + M_{zz}$; this is the expectation value of $J^2 \propto \vec{\sigma}^1 \cdot \vec{\sigma}^2$, and we name it the dipolar order. The quasiconserved quantities can also be analyzed by using the eigenspectrum of $\hat{\mathcal{L}}_{\text{sec}}$. It has four zero eigenvalues. One of the zero eigenvalues corresponds to the preservation of the trace. The three other zero eigenvalues correspond to the above three quasiconserved quantities.

While solving the equation, the initial condition is chosen as $M_{zz}|_{t\to 0} = M_\circ$ and other observables as zero. The solution of $M_{zz}(t)$ from Eq. (5) is given by

$$M_{zz}^{\text{pre}}(t) = \frac{M_\circ}{4}\left(1 - \frac{2\omega_1^2}{\kappa_1^2}(1 - \cos(\kappa_1 t)e^{-t\kappa_1^2\tau_c})\right), \qquad (10)$$

where $\kappa_1^2 = 4\omega_1^2 + 9\omega_{d_0}^2/4$. Therefore, $M_{zz}|_{t\to\infty} = \frac{M_\circ}{4}(1 - 2\omega_1^2/\kappa_1^2)$. The above solution shows that the initial transient phase oscillates with a frequency κ_1 and it reaches the prethermal steady state ($M_{zz}|_{t\to\infty}$) in a characteristic time-scale $T_{\text{pre}} = 1/(\tau_c\kappa_1^2)$. In Fig. 1, T_{pre} indicates the timescale of the system to reach the prethermal state from the initial transient phase.

B. Emergence of constrained thermalization

Next, we include $\hat{\mathcal{L}}_n \hat{\rho}_s$ in the dynamics, whose form in the Hilbert space is given by

$$\mathcal{L}_n \rho_s = -i[\mathcal{H}_{bs} + \mathcal{H}_{ds}, \rho_s] + \mathcal{D}_1 \rho_s + \mathcal{D}_2 \rho_s. \quad (11)$$

The shift terms are the Kramers-Kronig pairs of the second-order dissipative terms of the nonsecular parts. They result in the renormalization of the Zeeman frequency. $\mathcal{H}_{bs}$ is called the

Bloch-Siegert shift, $\mathcal{H}_{bs} = 2\omega_1^2 \omega_\circ \tau_c \mathcal{Z}(2) I_z^i$; similarly $\mathcal{H}_{ds}$ represents the second-order dipolar shift; the expression is given by $\mathcal{H}_{ds} = [\omega_{d_1}^2 \omega_\circ \tau_c \mathcal{Z}(1) + 2\omega_{d_2}^2 \omega_\circ \tau_c \mathcal{Z}(2)] I_z^i$. Here $\mathcal{Z}(m) = \tau_c/[1 + (m\omega_\circ \tau_c)^2]$. These shift terms do not contribute to the decay rate and minimally affect the steady-state configuration, so we ignore them in the rest of the analysis. The explicit forms of the dissipative operators in Eq. (11) can be written as

$$\mathcal{D}_1 \rho_s = \sum_{m=-2}^{2} |\omega_{d_m}|^2 \mathcal{Z}(m) \big[2\mathcal{T}_2^{-m} \rho_s \mathcal{T}_2^m - \big\{ \mathcal{T}_2^m \mathcal{T}_2^{-m}, \rho_s \big\} \big] \quad [\forall m \neq 0],$$

$$\mathcal{D}_2 \rho_s = \sum_{i,j=1}^{2} \omega_1^2 \mathcal{Z}(2) \big[2 I_\pm^i \rho_s I_\mp^j - \big\{ I_\mp^j I_\pm^i, \rho_s \big\} \big]. \quad (12)$$

We analyze the above Eq. (11) using the observables defined earlier in Eq. (4). The super-operator $\hat{\mathcal{L}}_{sec} + \hat{\mathcal{L}}_n$ has two zero eigenvalues. In the presence of the nonsecular terms, two of the earlier four quasiconserved quantities will no longer be conserved. The prethermal state does not survive in this regime, as $3\omega_{d_0}\dot{M}_{zz} + \omega_1 \dot{M}_x \neq 0$. Also, we have $\dot{M}_{xx} \neq 0$ and, $\dot{M}_{zz} + \dot{M}_{yy} \neq 0$. But the dipolar order still survives, $(\dot{M}_{xx} + \dot{M}_{yy} + \dot{M}_{zz} = 0)$. Therefore, this regime shows a constrained thermalization, as the initial memory partly survives. The resulting equation of the observables are

$$\dot{M}_x = -\big(2q_1 + \tfrac{5}{2}p_1 + p_2 \big) M_x + \text{terms in Eq. (6)}, \quad (13)$$

$$\dot{M}_{zz} = -(8q_1 + 2p_1) M_{zz} + (4q_1 + p_1)(M_{xx} + M_{yy}) + \text{terms in Eq. (7)}, \quad (14)$$

$$\dot{M}_{yy} = -(4q_1 + p_2 + p_1) M_{yy} + p_2 M_{xx} + (4q_1 + p_1) M_{zz} + \text{terms in Eq. (8)}, \quad (15)$$

$$\dot{M}_{xx} = -(4q_1 + p_2 + p_1) M_{xx} + p_2 M_{yy} + (4q_1 + p_1) M_{zz}. \quad (16)$$

Here $q_1 = \omega_1^2 \mathcal{Z}(2)$ and $p_m = |\omega_{d_m}|^2 \mathcal{Z}(m)$. In the limit of $\omega_\circ \tau_c \gg 1$, the solution of transverse magnetization mode $M_{zz}(t)$ is written as

$$M_{zz}(t) \approx \frac{M_\circ}{3} - e^{-t/T_\alpha} \left(\frac{M_\circ}{3} - M_{zz}^{pre}(t) \right),$$

$$\frac{1}{T_\alpha} = 3(p_1 + 4q_1). \quad (17)$$

Hence, the above solution of $M_{zz}(t)$ gives the notion of decay of prethermal order. T_α is the decay rate due to the nonsecular part.

The dynamics of the other observables connected to prethermal order and dipolar order $\{M_x, M_{xx}, M_{yy}, M_{zz}\}$ are also shown in Fig. 2(a). The observables $\{M_{yy}, M_{zz}\}$ get nonzero steady-state values in the prethermal time regime, and M_{xx} remains zero. Then at a later time, they begin to evolve. The constrained thermalization is shown in the time regime T_α of Fig. 1. The aforementioned terms in Eq. (11) give an effective decay in the dynamics. The decay time is denoted as T_α. The expression of the decay rate is given in Eq. (17). It is generally expressed as $1/T_\alpha \propto \frac{1/T_{pre}}{1+(\omega_\circ \tau_c)^2}$. If one begins with $M_x|_{t\to 0} \neq 0$ and other observables are zero, then it replicates the spin-locking phenomena in nuclear magnetic resonance (NMR) and the recent experiment by Beatrez *et al.* [18].

1. Existence of the critical limit

For a very weak system-bath interaction (long T_1 process), the timescale corresponding to the decay of quasiequilibrium state is denoted as $T_{1\rho}$ in the spin-temperature theory of

NMR [30]. In our case, T_α is equivalent to $T_{1\rho}$. The necessary condition for having a prethermal plateau is $T_\alpha \gg T_{pre}$. Therefore, to fulfill this condition, we must have $\omega_\circ \tau_c \gg 1$. In this limit, $1/T_{pre} \propto \tau_c$ and $1/T_\alpha \propto 1/\tau_c$.

It is known that in the case of the dynamics of a dissipative system, the eigenvalues of $\hat{\mathcal{L}}$ must lie in the nonpositive plane. The imaginary part of the eigenvalue comes from the unitary process due to the first-order terms and shift terms. On the other hand, the real part depicts the nonunitary dissipation [31]. The lifetime of the prethermal plateau is independent of the unitary process, so we neglect the imaginary part of the eigenvalue of $\hat{\mathcal{L}}$ for the rest of the analysis.

In this regime, $\hat{\mathcal{L}}$ has two zero eigenvalues. Others are the decaying modes. The decay times are obtained by the inverse of the modulus of the eigenvalues. In Fig. 2(b), we have plotted the modulus of the eigenvalues as a function of the dimensionless quantity $\omega_\circ \tau_c$. It shows that for $\omega_\circ \tau_c \gg 1$, two eigenvalues are much smaller than the others. When the remaining 12 modes decay, those two modes still remain alive and the system has a prethermal plateau of a finite lifetime, whereas for $\omega_\circ \tau_c \ll 1$, all the 14 modes decay nearly at the same time. Hence, the plateau will not survive in this regime.

The solution of $M_{zz}(t)$ as a function of time and for the specific choice of $\omega_\circ \tau_c$ is shown in the contour plot [Fig. 2(c)]. It depicts clearly a critical point at $\omega_\circ \tau_c = 1$. For $\omega_\circ \tau_c \gg 1$, there exist two distinct decay rates. The prethermal plateau is clearly visible in the regime. As we increase the value of $\omega_\circ \tau_c$, the length of the plateau increases as the differences between the eigenvalues grow. For $\omega_\circ \tau_c \ll 1$, the plateau ceases to
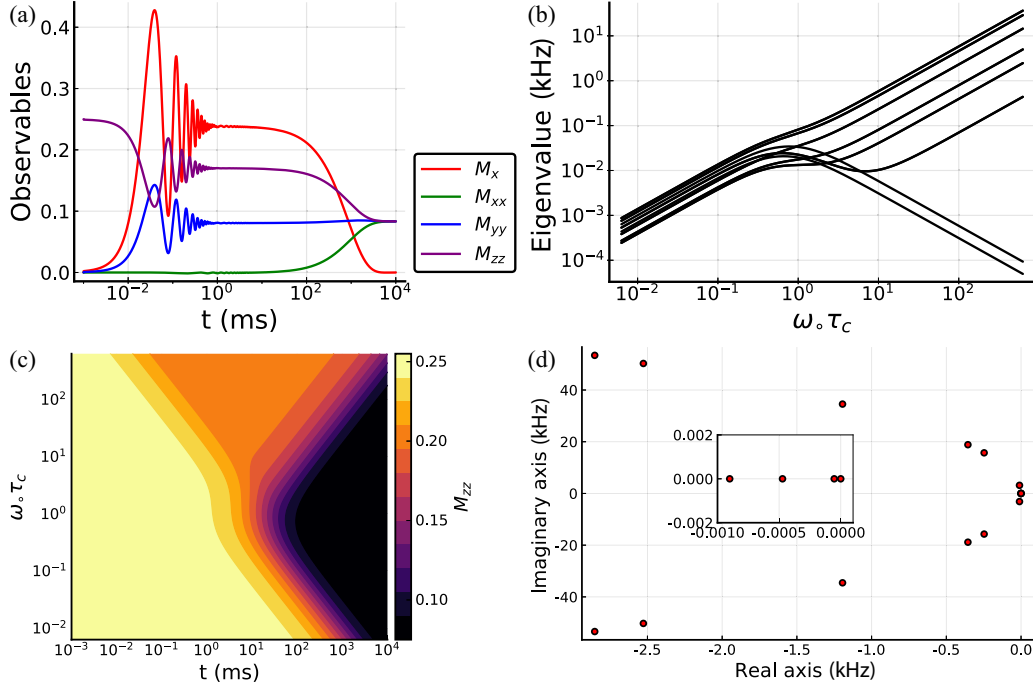
FIG. 2. Subfigure (a) shows the plots of the expectation values vs t. We show M_x in red (color online; the upper curve), M_{xx} in green (color online; the lower curve), M_{yy} in blue (color online; the second from the bottom), M_{zz} in purple (color online; the second from the top). All the plots are done by numerically solving Eqs. (5) and (11) simultaneously. The values of the parameters are given below: $\omega_1 = 2\pi \times 5$ KHz, $|\omega_{d_m}| = 2\pi \times 5$ kHz, $\omega_\circ = 2\pi \times 10$ MHz, $\tau_c = 1$ μs. It shows that in the intermediate timescale the prethermal order is preserved, but after a characteristic time it decays. First two eigenvalues of total $\hat{\mathcal{L}}$ (excluding $\mathcal{H}_{SL}$) are zero. Modulus of the other 14 eigenvalues are plotted as a function of $\omega_\circ \tau_c$ in subfigure (b). For $\omega_\circ \tau_c \gg 1$, the separate existence of the lowest two eigenstates from others is clearly visible, whereas for $\omega_\circ \tau_c \leqslant 1$, they merge. Subfigure (c) shows the filled contour of $M_{zz}(t)$ as a function of $\omega_\circ \tau_c$ and t. $\omega_\circ \tau_c \approx 1$ is the critical point of the dynamics. For $\omega_\circ \tau_c > 1$, the orange (color online; the gray region on the top) triangular region shows the prethermal plateau. For $\omega_\circ \tau_c < 1$, no such plateau forms. For subfigures (b) and (c), the effect of the imaginary part of the eigenvalues is neglected. Subfigure (d) shows the numerical plots for the distribution of the sixteen eigenvalues of $\hat{\mathcal{L}}_{sec} + \hat{\mathcal{L}}_n + \hat{\mathcal{L}}_{SL}$ in the real and imaginary axes. Here, $T_1 = 5 \times 10^4$ ms and $M_{th} = 0.6$. The lowest four eigenvalues are close to zero and are merged. The inset in the middle of the plot shows those four eigenvalues with an enlarged scale. The first two eigenvalues in the inset from the left are responsible for the prethermal plateau. The third one (from the left) shows the notion of constrained thermalization. The right one leads the system to the final steady state.

exist. This criticality is reminiscent of the behavior of the relaxation rates due to spin-lattice relaxation as a function $\omega_\circ \tau_c$, as reported by Bloembergen and others [32,33]. They found that for high motional narrowing, $\omega_\circ \tau_c \ll 1$, and for the other regime (large macromolecules or solids) $\omega_\circ \tau_c \gg 1$.

C. Emergence of unconstrained thermalization

For the chosen parameters, the effect of $\mathcal{H}_{SL}$ is prominent after the system reaches the unconstrained thermalization regime. The spectral density function for the system-local environment coupling is given by

$$P_\pm \pm i\delta\omega_\pm = \int_0^\infty d\tau \, \omega_{SL}^2 e^{-\tau/\tau_c} e^{\mp i(\omega_L - \omega_\circ)\tau} \text{Tr}_L\{L_\pm L_\mp \rho_L^{eq}\}. \tag{18}$$

We also assume here $\text{Tr}_L\{L_\pm L_\mp \rho_L^{eq}\} = 1 \pm M_{th}$. The assumption implies that the system will eventually inherit the equilibrium populations $(1 \pm M_{th})/2$, due to interaction with the local environment. Here M_{th} is the equilibrium polarization. So, $M_z^{eq} = M_{th}$. The form of $\hat{\mathcal{L}}_{SL}\hat{\rho}_s$ in the Hilbert space is given by

$$\mathcal{L}_{SL}\rho_s = -i[\mathcal{H}_{lamb}, \rho_s] + \mathcal{D}_3\rho_s. \tag{19}$$

$\mathcal{H}_{lamb}$ is known as Lamb shift. It has a minimal contribution to the steady state so we neglect it for further analysis. The expression is given by $\mathcal{H}_{lamb} = \sum_{i=1}^2 (\delta\omega_- I_+^i I_-^i - \delta\omega_+ I_-^i I_+^i)$. The form of $D_3\rho_s$ is given by

$$D_3\rho_s = \sum_{i=1}^2 P_\mp [2I_\pm^i \rho_s I_\pm^i - \{I_\pm^i I_\mp^i, \rho_s\}]. \tag{20}$$

In general, P_-, P_+ is defined as the probability of the downward and upward transition due to $\mathcal{H}_{SL}$ [34]. Here we define $P_+ + P_- = 1/T_1$. We also note that $M_{th} = \frac{P_- - P_+}{P_- + P_+}$. In terms of observables which are connected to the dipolar order, the above dynamical Eq. (19) can be written as

$$\dot{M}_x = -\frac{M_x}{T_1} + \text{terms in Eq. (13)}, \tag{21}$$

$$\dot{M}_{zz} = -\frac{4M_{zz}}{T_1} + \frac{M_z}{T_1} + \text{terms in Eq. (14)}, \tag{22}$$

$$\dot{M}_{yy} = -\frac{2M_{yy}}{T_1} + \text{terms in Eq. (15)}, \tag{23}$$

$$\dot{M}_{xx} = -\frac{2M_{xx}}{T_1} + \text{terms in Eq. (16)}, \tag{24}$$

$$\dot{M}_z = -\frac{2M_z}{T_1} + \frac{2M_{th}}{T_1}. \tag{25}$$

TABLE I. Comparison of different dynamical phases.

Dynamical phase	Liouvillian	Quasiconserved quantity	Dark state
Prethermalization	$\hat{\mathcal{L}}_{\mathrm{sec}}$	(a) $3\omega_{d_0} M_{zz} + \omega_1 M_x$,	All eigenstates
		(b) M_{xx}, (c) $M_{yy} + M_{zz}$	corresponding to (a)
Constrained thermalization	$\hat{\mathcal{L}}_{\mathrm{sec}} + \hat{\mathcal{L}}_n$	(a) $M_{xx} + M_{yy} + M_{zz}$	Only singlet state
Unconstrained thermalization	$\hat{\mathcal{L}}_{\mathrm{sec}} + \hat{\mathcal{L}}_n + \hat{\mathcal{L}}_{\mathrm{SL}}$	None	None

From the above Eq. (19), it is clear that the dipolar order is broken [$\dot{M}_{xx} + \dot{M}_{yy} + \dot{M}_{zz} \neq 0$] in the presence of $\mathcal{H}_{\mathrm{SL}}$. Excluding $\mathcal{H}_{\mathrm{DR}}(t)$, $\mathcal{H}_{\mathrm{DD}}$, the final steady-state density matrix is diagonal. For this case, the steady-state solution is given by $M_z|_{t\to\infty} = M_{\mathrm{th}}$, $M_{zz}|_{t\to\infty} = M_{\mathrm{th}}^2/4$, and the value of the other observables are zero.

IV. DISCUSSION

The total Liouvillian ($\hat{\mathcal{L}}$) has a single zero eigenvalue, which means the steady state is unique and it has no initial memory. Therefore, the system reaches a unique final steady state under the evolution of full $\mathcal{L}$. The distribution of the eigenvalues is plotted in Fig. 2(d). In the inset, the first three eigenvalues (from the left in the inset) decay at a longer timescale. Among them, the first two are responsible for the prethermal plateau, and the third one is for constrained thermalization, as only the dipolar mode survives after the prethermal state decays. The zero eigenvalue stands for the steady state; it appears when all 15 eigenmodes decay.

The decay rate of the dipolar order is much slower than the prethermal order. This kind of quasiconservation law was recently predicted by Peng *et al.* in kicked dipolar model [19]. For $T_\alpha \ll T_1$, there exists another plateau in the system, which is shown in Fig. 1. For $\omega_\circ \tau_c \ll 1$, [$T_\alpha \approx T_{\mathrm{pre}}$], the initial transient phase skips the prethermal plateau and directly goes to the second plateau, whereas for $T_1 \ll T_\alpha, T_{\mathrm{pre}}$, the system directly arrives at final the steady state, as there is no existence of prethermalization.

The cascaded dynamics can be analyzed by the existence of the dark states in each regime. The nonequilibrium steady state (ρ_∞) is defined as the null vector of the Liouvillian ($\mathcal{L}\rho_\infty = 0$). If ρ_∞ is a pure density matrix ($\rho_\infty = |\psi_\infty\rangle\langle\psi_\infty|$), then $|\psi_\infty\rangle$ is defined as dark state [35]. Here, in the prethermal regime, all the eigenstates of the observables corresponding to the prethermal order act as a dark state. When the prethermal plateau decays, three of the previous four states are no longer dark states. In the constrained thermalization regime, only the Bell singlet state ($\frac{1}{\sqrt{2}}(|10\rangle - |01\rangle)$) is acting as a dark state. Finally, when the system reaches unconstrained thermalization, there exists no dark state in the system. Table I shows the summary of the above description.

For any choice of initial state, the cascaded structure of the dynamics is qualitatively unchanged. In real experiments, one can prepare the possible initial state by analyzing the interacting Hamiltonians and the quasiconserved observables. For example, the prethermal order contains $\sum_{i=1}^{2} \sigma_x^i$. In the case of a dipolar system, initially polarized to Z direction, a $\pi/2$ pulse in the Y direction can make the system an eigenstate of $\sum_{i=1}^{2} \sigma_x^i$. For this choice of the initial state, prethermalization occurs in presence of an on-resonant periodic drive. This experiment is referred to as "spin locking" in NMR. Similarly, both the prethermal order and dipolar order contain $\sigma_z \otimes \sigma_z$. The eigenstate ($|\uparrow\uparrow\rangle$) corresponding to the maximum eigenvalue of that observable can be prepared by pumping all the atoms to the upper levels. Our results show the existence of a prethermal plateau for such an initial state. Similarly, other initial states may also be chosen to demonstrate the emergence of prethermalization plateau provided they are not dark states.

A long prethermal plateau is useful for designing sensitive magnetometers and quantum-sensors [18]. The necessary conditions for this are $T_{\mathrm{pre}} \ll T_\alpha \ll T_1$ and $\omega_\circ \tau_c \gg 1$. One can design a system to have a strong dipolar coupling and can apply a strong drive to achieve this condition at any given temperature. We show here the simple case of a dipolar-coupled two-spin system, whereas in the actual experiment a dipolar network is considered. Our results show good agreement with the recent experiments by Beatrez *et al.* and it can be extended to the dipolar network because the timescale separation between different interacting Hamiltonians and the cross-relaxation effects are also present in such cases. The steady-state value will change accordingly by increasing the number of atoms, which is beyond the interest of the paper. Motivated by these recently reported experiments, we have confined ourselves to the Markovian regime, where the environment and the system have largely separated timescale. We note that prethermalization can also be observed in the presence of non-Markovian dissipation if suitable quasiconserved quantities are present in the system. At lower temperature (higher τ_c), the non-Markovian effects in the cascaded dynamics can be demonstrated using solid-state NMR.

V. CONCLUSION

In summary, we present here the complete dynamical theory of periodically driven dissipative dipolar system using FRQME. We show that the journey to the equilibrium for such systems is a multistage process. The initial transient phase is governed by the first-order unitary processes. The second-order cross-relaxation process leads to the prethermal state. This prethermal state further decays due to the nonsecular part of the drive and dipolar Hamiltonian. We calculate an effective decay rate that predicts the lifetime of such a state. We show that there exists a critical limit to the temporal correlation of the local environmental fluctuation. Beyond the limit, the prethermal plateau does not survive. We also observe that there exists another quasiconserved quantity, even after the prethermal state vanishes. Finally, we discuss the effect of the system-bath coupling, which leads the system to the final steady state. The analysis in the above has been carried out using specific values of system parameters to demonstrate the

possible existence of multiple prethermal plateaus. However, we note that for strong system-environment coupling, there may not be a well-defined thermal plateau as the timescales of various may overlap with each other. We envisage that this theoretical exposition of complete dynamics of a driven dissipative dipolar system will pave the way to a better understanding of the thermalization problem.

[1] J. Berges, S. Borsanyi, and C. Wetterich, Phys. Rev. Lett. **93**, 142002 (2004).

[2] S. Sen, T. R. K. Mohan, and J. M. M. Pfannes, Phys. A (Amsterdam, Neth.) **342**, 336 (2004).

[3] J. M. Deutsch, Rep. Prog. Phys. **81**, 082001 (2018).

[4] M. Ueda, Nat. Rev. Phys. **2**, 669 (2020).

[5] J. M. Deutsch, Phys. Rev. A **43**, 2046 (1991).

[6] M. Srednicki, Phys. Rev. E **50**, 888 (1994).

[7] M. Srednicki, J. Phys. A: Math. Gen. **32**, 1163 (1999).

[8] T. Kuwahara, T. Mori, and K. Saito, Ann. Phys. **367**, 96 (2016).

[9] D. A. Abanin, W. De Roeck, and F. Huveneers, Phys. Rev. Lett. **115**, 256803 (2015).

[10] C. Fleckenstein and M. Bukov, Phys. Rev. B **103**, L140302 (2021).

[11] M. Holthaus, J. Phys. B: At., Mol. Opt. Phys. **49**, 013001 (2016).

[12] S. A. Weidinger and M. Knap, Sci. Rep. **7**, 45382 (2017).

[13] M. Bukov, S. Gopalakrishnan, M. Knap, and E. Demler, Phys. Rev. Lett. **115**, 205301 (2015).

[14] C. Yin, P. Peng, X. Huang, C. Ramanathan, and P. Cappellaro, Phys. Rev. B **103**, 054305 (2021).

[15] M. Bukov, L. D'Alessio, and A. Polkovnikov, Adv. Phys. **64**, 139 (2015).

[16] A. Rubio-Abadal, M. Ippoliti, S. Hollerith, D. Wei, J. Rui, S. L. Sondhi, V. Khemani, C. Gross, and I. Bloch, Phys. Rev. X **10**, 021044 (2020).

[17] K. Viebahn, J. Minguzzi, K. Sandholzer, A.-S. Walter, M. Sajnani, F. Gorg, and T. Esslinger, Phys. Rev. X **11**, 011057 (2021).

[18] W. Beatrez, O. Janes, A. Akkiraju, A. Pillai, A. Oddo, P. Reshetikhin, E. Druga, M. McAllister, M. Elo, B. Gilbert, D. Suter, and A. Ajoy, Phys. Rev. Lett. **127**, 170603 (2021).

[19] P. Peng, C. Yin, X. Huang, C. Ramanathan, and P. Cappellaro, Nat. Phys. **17**, 444 (2021).

[20] B. Neyenhuis, J. Zhang, P. W. Hess, J. Smith, A. C. Lee, P. Richerme, Z.-X. Gong, A. V. Gorshkov, and C. Monroe, Sci. Adv. **3**, e1700672 (2017).

[21] A. Chakrabarti and R. Bhattacharyya, Phys. Rev. A **97**, 063837 (2018).

[22] A. Chatterjee and R. Bhattacharyya, Phys. Rev. A **102**, 043111 (2020).

[23] N. Chanda and R. Bhattacharyya, Phys. Rev. A **104**, 022436 (2021).

[24] N. Chanda and R. Bhattacharyya, Phys. Rev. A **101**, 042326 (2020).

[25] S. Saha and R. Bhattacharyya, J. Magn. Resonance Open **10–11**, 100046 (2022).

[26] S. Saha and R. Bhattacharyya, J. Phys. B: At., Mol. Opt. Phys. **55**, 235501 (2022).

[27] A. Chakrabarti and R. Bhattacharyya, arXiv:1911.07607 (2019)

[28] A. Abragam, *The Principles of Nuclear Magnetism* (Oxford University Press, Oxford, UK, 1961).

[29] G. G. C. Cohen-Tannoudji and J. Dupont-Roc, *Atom-Photon Interactions: Basic Processes and Applications* (Wiley-VCH, Berlin, 1998).

[30] C. P. Slichter, *Principles of Magnetic Resonance*, 3rd ed. (Springer, Berlin, 1996).

[31] V. V. Albert and L. Jiang, Phys. Rev. A **89**, 022118 (2014).

[32] N. Bloembergen, E. M. Purcell, and R. V. Pound, Phys. Rev. **73**, 679 (1948).

[33] N. Bloembergen, E. M. Purcell, and R. V. Pound, Nature (London) **160**, 475 (1947).

[34] F. P. Heinz-Peter Breuer, *The Theory of Open Quantum Systems* (Oxford University Press, Oxford, UK, 2002).

[35] B. Buča and T. Prosen, New J. Phys. **14**, 073007 (2012).